

Structure and Energetics of Ionized Water Clusters: $(\text{H}_2\text{O})_n^+$, $n = 2-5$

R. N. Barnett and Uzi Landman*

School of Physics, Georgia Institute of Technology, Atlanta, Georgia 30332-0430

Received: September 6, 1996; In Final Form: October 23, 1996[⊗]

Energetics and geometrical structures of neutral, $(\text{H}_2\text{O})_n$, and ionized, $(\text{H}_2\text{O})_n^+$, water clusters, with $n = 2-5$, are investigated using local-spin-density functional electronic structure calculations with exchange-correlation gradient corrections. While the ground-state structures of the neutral clusters are hydrogen-bonded cyclic ones, those of the molecular ions are noncyclic. The lowest energy isomers of the ionized $(\text{H}_2\text{O})_n^+$ clusters contain a hydrazine-like fragment, $(\text{H}_2\text{OOH}_2)^+$, hydrogen-bonded to the extra water molecules. Higher energy isomers of the cluster ions are based on hydrogen bonding to a disproportionated fragment, $(\text{H}_3\text{O})^+\text{OH}$.

1. Introduction

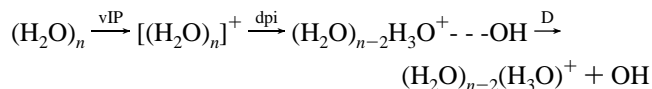
The properties of water clusters have been the subject of increasing research activities in recent years due to the ubiquity of H_2O as one of the most important polar solvents, as well as the importance of water clusters in atmospheric science. These studies include investigations of neutral water clusters,¹ $(\text{H}_2\text{O})_n$, electron attachment and localization modes (surface and interior states) in water clusters,^{1b,2} $(\text{H}_2\text{O})_n^-$ (see also investigations of $(\text{H}_2\text{O})_n^{-2}$ in ref 3), ionized clusters,⁴⁻⁸ i.e., $(\text{H}_2\text{O})_n^+$, and fragmentation processes occurring upon ionization,⁹⁻¹² as well as studies of ion and neutral hydration systems,^{9,13,14} i.e., $\text{X}(\text{H}_2\text{O})_n$ and $\text{X}(\text{H}_2\text{O})_n^\pm$, where X is a solvated species (atom or molecule), including protonated clusters,^{9,15} $(\text{H}_2\text{O})_n\text{H}^+$. Such studies provide insights into the nature of the hydrogen bonding and the rearrangement dynamics of hydrogen-bond networks, proton-transfer mechanisms, solvation phenomena, charging processes, and fundamental mechanisms underlying ion chemistry of the upper atmosphere.¹⁶

Mass spectra of water clusters are usually dominated by protonated cluster ions $(\text{H}_2\text{O})_n\text{H}^+$, which are produced by fast intracluster reactions during the ionization process. Indeed, protonated cluster ions have been observed as the major constituent in a weakly ionized gas containing at least trace amounts of water,^{5,18} as well as in flowing afterglows,¹⁹ in flames,²⁰ and in Earth's upper atmosphere.¹⁶ (The protonated dimer ion $(\text{H}_2\text{O})_2\text{H}^+$ plays an important role in the ion chemistry of the upper atmosphere, dominating the ion composition in the D region in the ionosphere.²¹) Furthermore, charged water species (such as the oxonium ion, H_3O^+ , and H_3O_2^+) occur often as solvated charge carriers in aqueous solutions, condensed phases (ices), and clusters (such as the celebrated $(\text{H}_2\text{O})_{21}\text{H}^+$ cluster,²² which may be described as $(\text{H}_2\text{O})_{20}\cdot\text{H}_3\text{O}^+$, i.e., an oxonium hydrated in a cage of 20 water molecules). Consequently, such species have been investigated extensively, experimentally and theoretically.^{9,23}

In contrast, experimental observations⁴⁻⁷ and theoretical investigations^{23,24} of unprotonated $(\text{H}_2\text{O})_n^+$ cluster ions are scarce. Early photoionization studies⁷ of $(\text{H}_2\text{O})_2$ have detected a low signal of $(\text{H}_2\text{O})_2^+$ near threshold and have determined an upper bound of the dimer adiabatic ionization potential $\text{aIP}[(\text{H}_2\text{O})_2] \leq 11.21 \pm 0.09$ eV (a lower value of 10.81–10.90 eV has been recently suggested⁸). Later He I photoelectron measurements¹⁸ determined the vertical ionization potential $\text{vIP}\{(\text{H}_2\text{O})_2\} = 12.1 \pm 0.1$ eV. Trimer ions, $(\text{H}_2\text{O})_3^+$, have been observed⁴ (with an intensity of 1% of the $\text{H}_3\text{O}^+(\text{H}_2\text{O})$ signal) in low-energy electron impact (15 eV) measurements, and larger

cluster ions, $(\text{H}_2\text{O})_n^+$, have been observed (for n up to 8) using a special supersonic ion beam source⁵ and by photoionization of neutral $\text{Ar}_m(\text{H}_2\text{O})_n$ clusters⁶ (for n up to 10). However, no evidence pertaining to the structures of unprotonated ionized water clusters has been given in these experimental studies.

The difficulty of observing unprotonated water cluster ions is attributed^{12,25} to the large configurational differences between the parent neutrals and the ionized clusters, which result in small Franck–Condon factors between the minima of the hypersurfaces of the two. Consequently, the vertically ionized cluster is formed in a highly vibrationally excited state, leading to dissociation. From theoretical studies of the ionization of $(\text{H}_2\text{O})_2$ it was concluded¹² that the ${}^2\text{A}''$ vertically ionized cation $[(\text{H}_2\text{O})_2]^+$ (in the following square brackets surrounding the molecule denote a vertically ionized state) can undergo a fast (simulated¹² to be about 50 fs) barrierless “autoprotonation” process induced by the charge imbalance due to the localized ionization hole on the proton donor, involving a significant contraction of the interoxygen distance, and resulting in a disproportionated ion (dpi), $\text{OH}(\text{H}_3\text{O}^+)$, where $d_{\text{OO}} = 2.502$ Å, compared to 2.957 Å in $(\text{H}_2\text{O})_2$ (see Figure 1 and Table 1). Excess energy in the ionized cluster may lead to dissociation of the dpi state into $\text{OH} + \text{H}_3\text{O}^+$, with a calculated endothermicity of ~ 1 eV. (We note here¹² that the energy of the vertically ionized state, $[(\text{H}_2\text{O})_2]^+$, exceeds that of the $\text{OH} + \text{H}_3\text{O}^+$ dissociation limit by 0.08 eV.) Generalization of the above sequence to larger clusters⁶ leads to the following scheme:



where vIP, dpi, and D denote the vertical ionization, disproportionation, and dissociation processes, respectively. Therefore, observation of the unprotonated ionized cluster $(\text{H}_2\text{O})_n^+$ requires that its energy be reduced sufficiently to prevent dissociation, such as via the evaporation of argon atoms in the experiments involving photoionization of $\text{Ar}_m(\text{H}_2\text{O})_n$ clusters.⁶ Similarly the gas-phase association reaction $(\text{H}_2\text{O})_n + \text{H}_2\text{O}^+ \rightarrow (\text{H}_2\text{O})_{n+1}^+$ requires effective energy transfer to the cold expanding gas, as in the experiments involving injected H_2O^+ ions into a supersonic water expansion.⁵

While the dpi, $(\text{H}_3\text{O})^+\text{OH}$, state of the ionized water dimer was invoked in the above discussion, recent investigation of pathways and dynamics of dissociation of ionized $(\text{H}_2\text{O})_2$ have revealed¹² that it is not the lowest ground-state configuration of the water dimer cation. Rather, these local-spin-density functional (LSD) calculations (including generalized exchange-

[⊗] Abstract published in *Advance ACS Abstracts*, December 15, 1996.

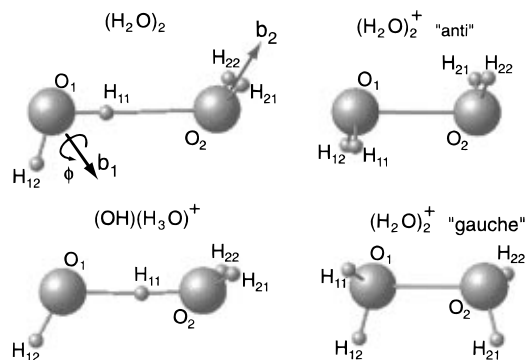


Figure 1. Optimized configurations (calculated at the GGC level) of the ground-state neutral water dimer, $(\text{H}_2\text{O})_2$, the hydrazine-like ground state of the dimer cation $(\text{H}_2\text{O})_2^+$ (a) (marked “anti”) and of the $(\text{H}_2\text{O})_2^+$ (g) (marked “gauche”), and disproportionated ion, $(\text{OH})(\text{H}_3\text{O})^+$, isomers. Large and small spheres denote oxygen and hydrogen atoms, respectively. Geometrical parameters are given in Table 1.

TABLE 1: Geometrical Parameters (Distances in Angstroms and Angles in Degrees) of the Optimal Structures (Calculated with a Plane-Wave Cutoff Energy of 158 Ry) for the Neutral Dimer, $(\text{H}_2\text{O})_2$, the Singly Charged Dimer Cation in the Disproportionate Ion Configuration, $(\text{OH})(\text{H}_3\text{O})^+$, the (a) Ground-State Hydrazine-like Configuration, and the (g) Isomer^a

	$(\text{H}_2\text{O})_2^+$			
	$(\text{H}_2\text{O})_2$	$(\text{OH})(\text{H}_3\text{O})^+$	(a)	(g)
Distances (Å)				
H_{11}O_1	0.976	1.409	0.981	0.980
H_{12}O^1	0.962	0.987	0.981	0.977
H_{21}O_2	0.965	0.971	0.981	0.980
H_{22}O_2	0.965	0.971	0.981	0.977
O_1O_2	2.957	2.502	2.176	2.182
H_{11}O_2	1.982	1.095		
Angles (deg)				
$\angle(\text{H}_{11}\text{O}_1\text{H}_{12})$	104.2	117.3	104.5	107.9
$\angle(\text{B}_1\text{O}_1\text{O}_2)$	125.7	119.7	97.3	105.5
ϕ_1	0.0	0.0	90.0	79.8
$\angle(\text{H}_{21}\text{O}_2\text{H}_{22})$	104.7	112.5	104.5	107.9
$\angle(\text{B}_2\text{O}_2\text{O}_1)$	124.0	144.1	97.3	105.5
ϕ_2	90.0	90.0	90.0	79.8
$\angle(\text{O}_2\text{O}_1\text{H}_{11})$			94.5	91.1
$\angle(\text{O}_2\text{O}_1\text{H}_{12})$			94.5	107.1
$\angle(\text{O}_1\text{H}_{11}\text{O}_2)$	177.0	176.0		
Dihedral Angles (deg)				
$\text{B}_1\text{O}_1\text{B}_2$	180.0	180.0	180.0	104.5
$\text{H}_{11}\text{O}_1\text{O}_2\text{H}_{22}$			180.0	100.9

^a Points B_1 (or B_2) are on the b_1 (or b_2) vector defined as the vector in the corresponding HOH plane, whose origin is on the oxygen (O_1 or O_2), and bisecting the corresponding $\angle(\text{HOH})$ angle (see Figure 1). ϕ_1 (or ϕ_2) is the angle (see Figure 1) required in order to rotate the corresponding water molecule (1 or 2) about its b vector (defined above), so that the HOH plane of the molecule coincides with the corresponding BO_1O_2 plane.

correlation gradient corrections, GGC) predicted that an ionized dimer with a hydrazine-like configuration²⁶ is lower than the dpi state by 0.22 eV (see $(\text{H}_2\text{O})_2^+$ (a) in Figure 1). In this state the dipoles of the H_2O molecules are oriented antiparallel to each other, the oxygens are bonded directly with a bond length $d_{\text{OO}} = 2.176$ Å (compared to 2.502 Å in the dpi isomer), and the ionization hole is delocalized, unlike the case of $(\text{H}_3\text{O}^+)-\text{OH}$, where it is localized on the oxonium part. In addition to the $(\text{H}_2\text{O})_2^+$ (a) ground state, a slightly higher in energy (0.02 eV) isomer was found with the two water molecules of the dimer cation in a “gauche” relative orientation (denoted as $(\text{H}_2\text{O})_2^+$ (g); see Figure 1). It is likely that the transformation from the neutral dimer configuration to that of $(\text{H}_2\text{O})_2^+$ (a) involves a barrier due to the significant rearrangement of the nuclei.

Dissociation of the water dimer may occur via alternative channels:¹² (i) the “oxonium channel” (O), $(\text{H}_2\text{O})_2 + h\nu \rightarrow \text{H}_3\text{O}^+ + \text{OH} + e^-$, and (ii) the “water channel” (W), $(\text{H}_2\text{O})_2 + h\nu \rightarrow \text{H}_2\text{O}^+ + \text{H}_2\text{O} + e^-$. The calculated energies required for dissociative ionization through these channels are $E_d(\text{O}) = 11.67$ eV (compared to 11.73 eV determined from the photoion yield curve⁷), and $E_d(\text{W}) = 12.75$ eV (compared to the experimentally estimated²⁵ value of 12.86 eV). We also note (see Figure 2 in ref 12) that while the vertically ionized state, $[(\text{H}_2\text{O})_2]^+$, may dissociate spontaneously into the O channel, its dissociation into the W channel requires an energy of 1.01 eV.

If the vertically ionized dimer relaxes into the ground state of the $\text{OH}(\text{H}_3\text{O})^+$ dpi isomer, dissociation into the O channel requires an energy of 1.02 eV (compared to an experimentally estimated⁷ lower bound of 0.6 eV), and dissociation into the W channel requires 2.11 eV (compared to an experimental lower bound⁷ of 1.6–1.7 eV). On the other hand, the vertically ionized dimer may relax into the $(\text{H}_2\text{O})_2^+$ (a), ground state, or the $(\text{H}_2\text{O})_2^+$ (g) isomer, in a process entailing a large configurational change and involving a barrier, or conversion between the dpi and the a or g isomers may occur, involving a barrier of ~ 0.2 eV (the barrier for the reverse transformation is ~ 0.42 eV); indeed Born–Oppenheimer (BO)–LSD–molecular dynamics (MD) simulations of the $(\text{OH})\text{H}_3\text{O}^+$ isomer thermalized at 150, 300, and 600 K have shown¹² that at the higher temperature, following several back-and-forth proton-transfer events, a vibrationally excited $(\text{H}_2\text{O})_2^+$ (a) state was formed. Dissociation of the (a) state into the W and O channels requires dissociation energies of 2.34 and 1.25 eV, respectively. From the above we conclude that the O channel is energetically favorable and will dominate for cold parent dimers and low (near threshold) ionization energies. However, dissociation into the W channel may occur for higher excitation energies.

In light of the above we focus in this paper on the energetics and structures of neutral $(\text{H}_2\text{O})_n$ and unprotonated ionized $(\text{H}_2\text{O})_n^+$ clusters, with $n \leq 5$. The main findings of our studies are that while neutral $(\text{H}_2\text{O})_n$ clusters, with $n = 3, 4$, and 5, form ground-state quasi-planar cyclic (polygonal) structures with each monomer acting as both a single donor and single acceptor, the ground-state structures of the ionized clusters are noncyclic, with chainlike structures containing a hydrazine-like fragment, $(\text{H}_2\text{O}-\text{OH}_2)^+$, being the energetically optimal ones. Molecular ion isomers containing an oxonium fragment, $(\text{H}_3\text{O}^+)\text{OH}$, are higher in energy (~ 0.1 eV), and the cyclic $(\text{H}_2\text{O})_n^+$ structures are energetically unfavorable by a larger amount (~ 0.5 – 0.6 eV higher in energy than the chainlike structures). Following a brief description in section 2 of the computational method, we present our results in section 3 and summarize them in section 4.

2. Method

In calculations of the total energies, structural optimization, and molecular dynamics simulations,¹² we have used our Born–Oppenheimer (BO) local-spin-density functional (LSD) molecular dynamics (MD) method²⁷ (BO–LSD–MD). In electronic structure calculations we have used nonlocal norm-conserving pseudopotentials²⁸ for the valence electrons of the oxygen atoms (s- and p-components, with s-nonlocality) and a local pseudopotential for the hydrogens. Exchange–correlation gradient corrections (GGC; with the exchange gradient correction of Becke²⁹ and the correlation gradient of Perdew³⁰) were included self-consistently.

As discussed in detail elsewhere,²⁷ in our method no supercells (i.e., periodic replicas of the ionic system) are used, thus allowing studies of charged and multipolar clusters in an accurate and straightforward manner. In dynamical simulations

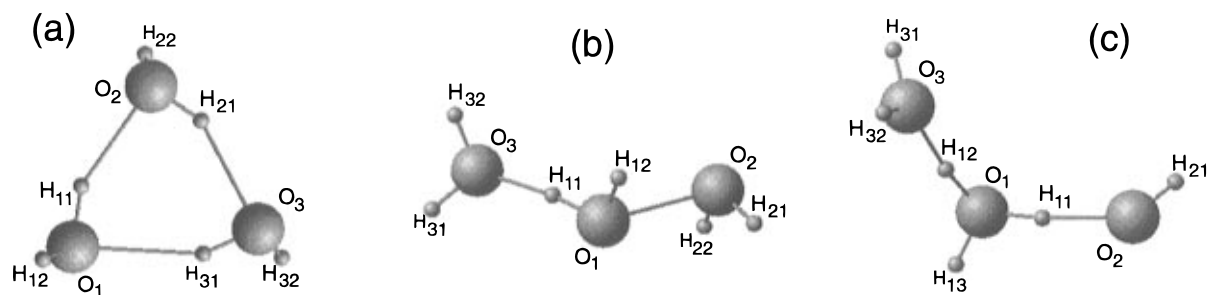


Figure 2. Optimized configurations of the ground state of neutral $(\text{H}_2\text{O})_3$ (a) and of the chainlike $(\text{H}_2\text{O})_3^+$ (b) and the $(\text{H}_2\text{O})_3^+(\text{dpi})$ isomers. Large and small spheres denote oxygen and hydrogen atoms. Geometrical parameters are given in Table 2a.

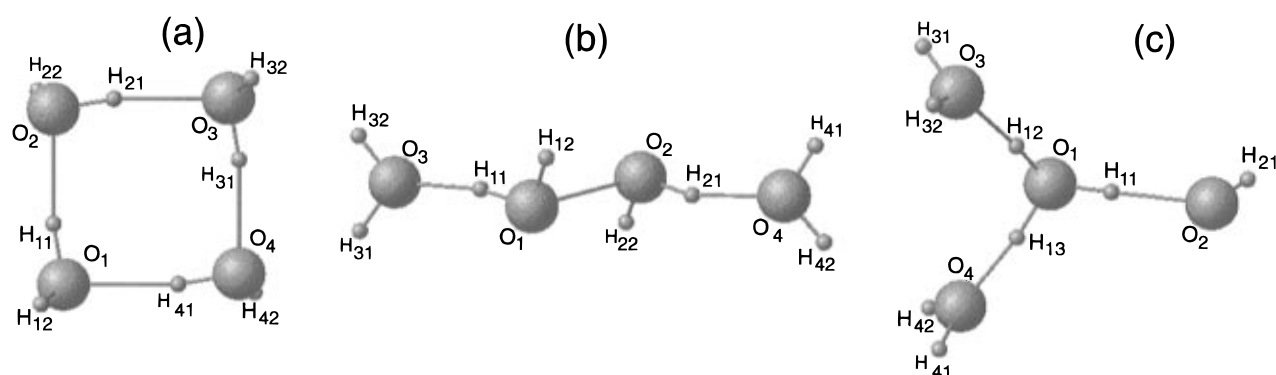


Figure 3. Same as Figure 2 but for the neutral and singly charged water tetramer. Geometrical parameters are given in Table 2b.

the Hellman–Feynman forces on the ions are evaluated between each MD step, involving iterative solution of the LS Kohn–Sham equations, thus ensuring that the ionic trajectories are followed on the BO potential energy surface. In the calculations for neutral and charged $(\text{H}_2\text{O})_n$ clusters a plane-wave cutoff of 96 Ry was used (for $n = 2$ we quote also results from our earlier calculations,¹² where a larger value, i.e., 158 Ry, has been used). A typical time step $\Delta t = 0.3$ fs was used in integration of the ionic equations of motion.

3. Energetics and Structures of $(\text{H}_2\text{O})_n$ and $(\text{H}_2\text{O})_n^+$, for $n \leq 5$

(a) Neutral $(\text{H}_2\text{O})_n$, $n = 2–5$ Clusters. The optimal structures for neutral $(\text{H}_2\text{O})_n$ clusters and for their cations $(\text{H}_2\text{O})_n^+$ with $n \leq 5$ are shown in Figure 1 (for $n = 2$) and Figures 2–4 (for $n > 2$), and their corresponding geometrical parameters are given in Table 1 (for $n = 2$) and Table 2 (for $n > 2$). The energetics of these clusters are given in Table 3.

In the neutral $(\text{H}_2\text{O})_n$ clusters (Figures 1, 2a, 3a, and 4a) the molecules are hydrogen-bonded and for the trimer, tetramer, and heptamer their ground-state structures are cyclic, close to planar, polygons^{1a} (for $(\text{H}_2\text{O})_4$ the oxygen marked O_4 in Figure 3a is located 0.090 Å above the $\text{O}_1\text{–O}_2\text{–O}_3$ plane, and for $(\text{H}_2\text{O})_5$ the oxygens marked O_1 and O_4 in Figure 4a are located in 1.0 and 0.8 Å, respectively, above the $\text{O}_2\text{–O}_3\text{–O}_5$ plane). In the tetramer all the H_2O molecules are equivalent to each other and the directions of their dipoles (being approximately along the bisector of the intermolecular H–O–H angle) alternate above and below the plane of the cluster, while for the odd numbered clusters not all molecules are equivalent since such cyclic alternation around the polygon cannot be completed.

The angles formed between the oxygens in these structures are close to the ideal polygonal ones (i.e., $(n - 2) 180^\circ/n$), and the distances between neighboring oxygens are shorter than in the dimer molecule ($d_{\text{OO}} = 2.957$ Å), with their average values being 2.890, 2.798, and 2.778 Å for $n = 3, 4,$ and 5 , respectively, in good agreement with experimentally determined values^{1a,31–34} (2.976, 2.90, 2.78, and 2.76 Å for $n = 2–5$, respectively),

superior to that obtained by previous high-level quantum chemistry ab initio calculations (see comparisons and citations in refs 1a, 31–34) and overall in somewhat better agreement with experiments than recent gradient-corrected density functional calculations (see ref 35, where $d_{\text{OO}} = 2.926, 2.789,$ and 2.683 Å is given for $n = 2, 3,$ and 4). The shortening of the O–O distances is associated (for $n = 4$ and 5) with a decrease in the distances between the (donor) hydrogens (H_d) and the acceptor (O_a) oxygen atoms hydrogen bonds, $\text{O}_d\text{–H}_d\cdots\text{O}_a$ (with average values of 1.825 and 1.795 Å for $n = 4$ and 5 compared to 1.982 Å in the dimer; in the trimer two of these distances are relatively short, i.e., 1.947 and 1.961 Å and one is longer, 2.085 Å, see Table 2a). At the same time $\text{O}_d\text{–H}_d$ bonds in the donor molecules in these clusters tend to elongate^{1a} compared to that in the dimer (0.976 Å), with average values of 0.982 and 0.984 Å for $n = 4$ and 5 . Additionally, these structures exhibit a larger degree of nonlinearity of the hydrogen bonds (i.e., the angle $\angle(\text{O}_d\text{–H}_d\cdots\text{O}_a)$) compared to that in the dimer (177°), having average values of $152^\circ, 170^\circ,$ and 176° for $n = 3, 4,$ and 5 , respectively, and showing a trend of decreased hydrogen-bond nonlinearity for larger clusters (with $n > 2$). The shortening of the O–O distances is also correlated with the monotonic increase with n of the binding energy (see E_b in Table 3, $E_b = E((\text{H}_2\text{O})_n) - nE(\text{H}_2\text{O})$) and consequently an increase of the hydrogen-bond energy (see E_{HB} in Table 3; $E_{\text{HB}} = E_b/n_{\text{HB}}$, where n_{HB} is the number of hydrogen bonds in the cluster). The pattern of increase of E_{HB} indicates nonadditivity effects suggesting that simple pair-potentials cannot provide accurate descriptions of the geometries of such small water clusters.³⁵

The relative stability of the water tetramer cluster, which as aforementioned is characterized by a cyclic alternation of the molecular dipole directions, is portrayed by the relatively large value of the H_2O removal energy calculated for it (see $\Delta(\text{H}_2\text{O})$ in Table 3; $\Delta(\text{H}_2\text{O}) = E((\text{H}_2\text{O})_n) - E((\text{H}_2\text{O})_{n-1}) - E(\text{H}_2\text{O})$) and the relative ease of H_2O removal from the pentamer cluster. The relatively high value of $\Delta(\text{H}_2\text{O})$ for the trimer is related to the fact that upon removal of a water molecule from this cluster

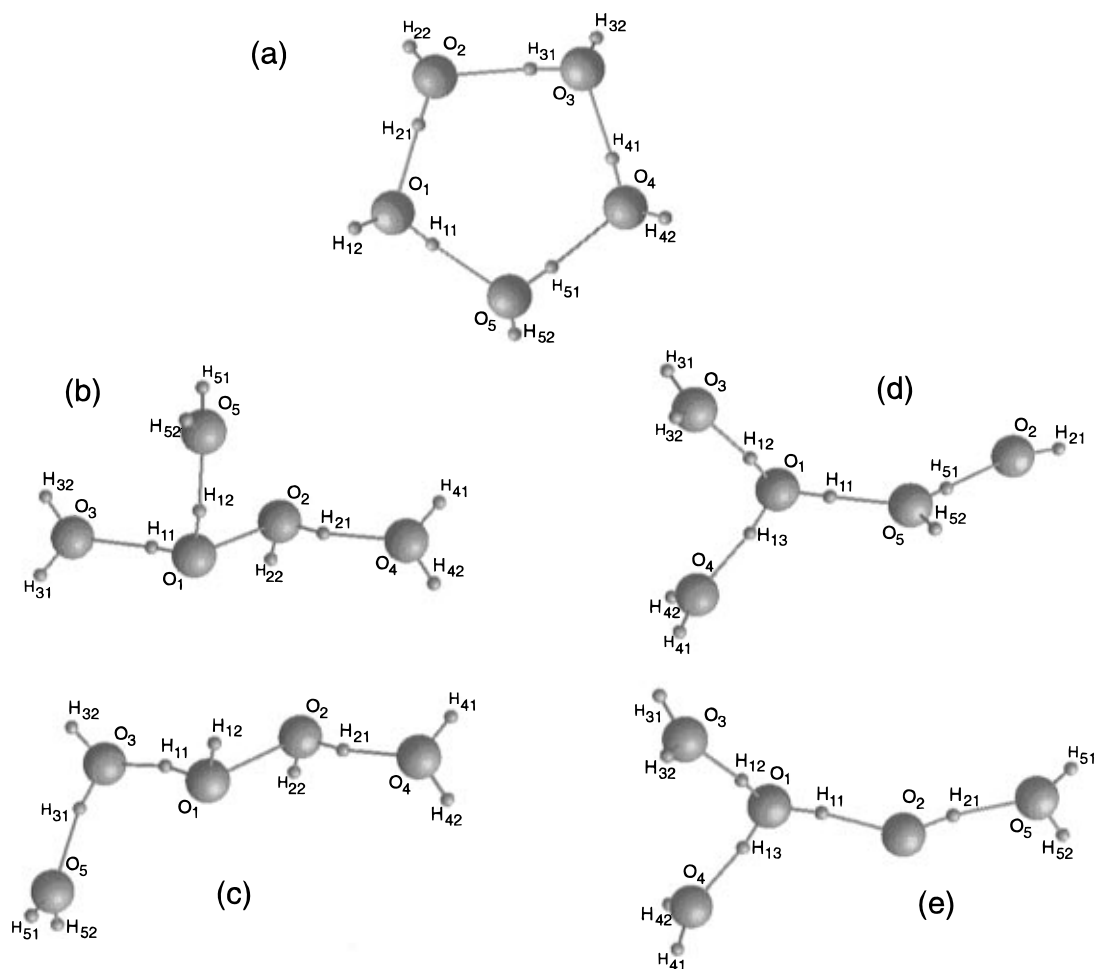


Figure 4. Same as Figure 2 but for the neutral and singly charged water pentamer. The neutral $(\text{H}_2\text{O})_5$ geometry is shown in part a, the geometries of two “hydrazine-based” isomers, $(\text{H}_2\text{O})_5^+(\text{aI})$ and $(\text{H}_2\text{O})_5^+(\text{aII})$, are shown in parts b and c, and the geometries of two “disproportionated ion-based” isomers, $(\text{H}_2\text{O})_5^+(\text{dpiI})$ and $(\text{H}_2\text{O})_5^+(\text{dpiII})$, are shown in parts d and e. Geometrical parameters are given in Table 2c.

to form the dimer, the number of hydrogen bonds is reduced from three to one.

(b) Ionized $(\text{H}_2\text{O})_n^+$, $n = 2-5$, Clusters. As noted already in the Introduction, we have found recently that a hydrazine-like structure $(\text{H}_2\text{O})_2^+(\text{a})$ in Figure 1) is a stable ground state of the ionized dimer with an energy 0.2 eV lower than the disproportionated ion, $(\text{H}_3\text{O})^+(\text{OH})$ isomer. The main result of the present study is that the lowest energy isomers of the larger molecular water cations $(\text{H}_2\text{O})_n^+$, $2 < n < 5$, whose neutral parents form cyclic ringlike structures, are noncyclic with the lowest energy corresponding to chainlike ones containing a hydrazine-like component (see Figures 2b, 3b, and 4b,c). For the pentamer cluster ions we show two isomers for the (a) and (dpi) motifs; in descending order of stability these are denoted as: (aI) corresponding to $(\text{H}_2\text{O})_2(\text{H}_2\text{OOH}_2)^+(\text{H}_2\text{O})$, where the two H_2O molecules on the left are hydrogen-bonded directly to one of the H_2O molecules of the hydrazine fragment; (aII) corresponding to $(\text{H}_2\text{O})(\text{H}_2\text{O})(\text{H}_2\text{OOH}_2)^+(\text{H}_2\text{O})$, where only one H_2O molecule is hydrogen-bonded directly to each of the molecules of the hydrazine fragment; (dpiI) corresponding to $(\text{H}_2\text{O})_2(\text{H}_3\text{O})^+(\text{H}_2\text{O})\text{OH}$, where the oxonium fragment is 3-fold hydrogen-bonded to water molecules; (dpiII) corresponding to $(\text{H}_2\text{O})_2(\text{H}_3\text{O})^+(\text{OH})(\text{H}_2\text{O})$, where the oxonium fragment is hydrogen-bonded directly to only two water molecules.

The vertical ionization potentials (vIP in Table 3) of the $(\text{H}_2\text{O})_n$ clusters show a monotonic decreasing trend with increasing n , and the reorganization energies ($E_R = \text{vIP}(\text{H}_2\text{O})_n - \text{aIP}(\text{H}_2\text{O})_n$) upon structural relaxation of the ionized clusters are rather significant (compare values in Table 3 to the single water molecule, where both measurements and calculations

show a relatively small $E_R \approx 0.1$ eV); relaxations of the molecular cations into cyclic structures result in higher energy isomers than the noncyclic ones, with corresponding larger aIP values (for example, the aIP of $(\text{H}_2\text{O})_3$ to form a cyclic molecular ion is 10.48 eV, and that for $(\text{H}_2\text{O})_4$ is 10.28 eV, the latter value calculated at the PLSD level, that is, including exchange-correlation gradient corrections, but using the wave functions and geometry obtained from LSD calculations). For all cases studied here the molecular ion clusters based on a hydrazine-like component (denoted as $(\text{H}_2\text{O})_n^+(\text{a})$) are more stable (i.e., lower aIP values) than the ones containing a disproportionated ion (dpi), with an energy difference of ~ 0.1 eV.

In the ionized clusters the distances between hydrogen-bonded oxygens are smaller than in the corresponding neutral ones (i.e., 2.472 and 2.426 Å in the (a) and (dpi) states of $(\text{H}_2\text{O})_3^+$, compared to 2.890 Å in the neutral; 2.570 and 2.493 Å in the (a) and (dpi) states of $(\text{H}_2\text{O})_4^+$, compared to 2.798 Å in the neutral; and the values in the range of $\sim 2.5-2.65$ Å in the $(\text{H}_2\text{O})_5^+$ isomers compared to an average distance of 2.778 Å in the neutral). Additionally, in general the hydrogen bonds in the ionized clusters are closer to linear than in the neutral parents. These results correlate with increased values for the water removal energies from the cluster ions ($\Delta^+(\text{H}_2\text{O}) = E(\text{H}_2\text{O})_n^+ - E(\text{H}_2\text{O})_{n-1}^+ - E(\text{H}_2\text{O})$), compared to those for the corresponding neutrals (compare $\Delta(\text{H}_2\text{O})$ and $\Delta^+(\text{H}_2\text{O})$ in Table 3).

4. Summary

In this paper the energetics and structures of neutral, $(\text{H}_2\text{O})_n$, and singly charged $(\text{H}_2\text{O})_n^+$, water clusters, with $n \leq 5$ were

TABLE 2: Geometrical Parameters (Distances in Angstroms and Angles in Degrees) of the Optimal Structures of Neutral and Singly Charged Isomers of Water Clusters^a

a											
	(H ₂ O) ₃	(H ₂ O) ₃ ⁺ (a)	(H ₂ O) ₃ ⁺ (dpi)		(H ₂ O) ₃	(H ₂ O) ₃ ⁺ (a)	(H ₂ O) ₃ ⁺ (dpi)				
Distances (Å)											
H ₁₁ O ₁	0.974	1.055	1.075	H ₂₁ O ₃	1.961						
H ₁₂ O ₁	0.958	0.971	1.070	H ₁₁ O ₃		1.425					
H ₁₃ O ₁			0.963	H ₁₂ O ₃					1.361		
H ₁₁ O ₂	1.947		1.562	O ₁ O ₂	2.848	2.153			2.570		
H ₂₁ O ₂	0.973	0.973	0.979	O ₂ O ₃	2.842						
H ₃₁ O ₃	0.971	0.961	0.961	O ₃ O ₁	2.981	2.472			2.426		
Angles (deg)											
∠(O ₁ H ₁₁ O ₂)	153			∠(H ₂₁ O ₂ H ₂₂)	106.6	105.3					
∠(O ₂ H ₂₁ O ₃)	149			∠(H ₃₁ O ₃ H ₃₂)	105.9	108.7			109.7		
∠(O ₃ H ₃₁ O ₁)	153			∠(H ₁₁ O ₂ H ₂₁)					116.4		
∠(O ₃ H ₁₂ O ₁)			109.7	∠(O ₁ O ₂ O ₃)	63.2						
∠(O ₁ H ₁₁ O ₃)		170.3		∠(O ₂ O ₃ O ₁)	58.5						
∠(H ₁₁ O ₁ H ₁₂)	105.9	106.4	111.5	∠(O ₃ O ₁ O ₂)	58.3	107.6			102.7		
b											
	(H ₂ O) ₄	(H ₂ O) ₄ ⁺ (a)	(H ₂ O) ₄ ⁺ (dpi)		(H ₂ O) ₄	(H ₂ O) ₄ ⁺ (a)	(H ₂ O) ₄ ⁺ (dpi)				
Distances (Å)											
H ₁₁ O ₁	0.982	1.022	1.00	H ₁₂ O ₃					1.473		
H ₁₂ O ₁	0.960	0.970	1.026	H ₁₃ O ₄					1.472		
H ₁₃ O ₁			1.026	O ₁ O ₂	2.798	2.214			2.614		
H ₁₁ O ₂	1.825		1.614	O ₁ O ₃		2.570			2.493		
H ₃₁ O ₃	0.960	0.963	0.960	O ₁ O ₄					2.493		
H ₁₁ O ₃		1.565									
Angles (deg)											
∠(O ₁ H ₁₁ O ₂)	170.5		178.4	∠(H ₁₂ O ₁ H ₁₃)					109.9		
∠(O ₁ H ₁₁ O ₃)		166.3		∠(O ₁ O ₂ O ₃)	89.9						
∠(O ₁ H ₁₂ O ₃)			172.6	∠(O ₂ O ₁ O ₃)		111.8			120.6		
∠(H ₁₁ O ₁ H ₁₂)	104.4	106.7	115.9	∠(O ₃ O ₁ O ₄)					103.2		
∠(H ₃₁ O ₃ H ₃₂)	104.4	106.9	108.2								
c											
	(H ₂ O) ₅	(H ₂ O) ₅ ⁺ (aI)	(H ₂ O) ₅ ⁺ (aII)	(H ₂ O) ₅ ⁺ (dpiI)	(H ₂ O) ₅ ⁺ (dpiII)		(H ₂ O) ₅	(H ₂ O) ₅ ⁺ (aI)	(H ₂ O) ₅ ⁺ (aII)	(H ₂ O) ₅ ⁺ (dpiI)	(H ₂ O) ₅ ⁺ (dpiII)
Distances (Å)											
H ₁₁ O ₁	0.986	1.006	1.058	1.028	1.011	H ₁₂ O ₅		1.661			
H ₁₂ O ₁	0.959	1.006	0.968	1.028	1.011	H ₃₁ O ₅			1.688		
H ₁₃ O ₁				1.007	1.010	H ₁₁ O ₅	1.783			1.557	
H ₂₁ O ₁	1.772					H ₂₁ O ₅					1.661
H ₂₁ O ₂	0.985	1.006	1.011	0.975	1.011	O ₁ O ₂	2.756	2.182	2.219		2.634
H ₁₁ O ₂					1.630	O ₁ O ₃		2.723	2.481	2.617	2.626
H ₃₁ O ₂	1.804					O ₁ O ₄				2.617	2.651
H ₃₁ O ₃	0.984	0.959	0.990		0.959	O ₁ O ₅	2.767	2.665		2.584	
H ₄₁ O ₃	1.812					O ₂ O ₃	2.786				
H ₁₁ O ₃		1.726	1.441			O ₂ O ₄		2.714	2.648		
H ₁₂ O ₃					1.631	O ₂ O ₅				2.845	2.655
H ₄₁ O ₄	0.982	0.959	0.962	0.959	0.959	O ₃ O ₄	2.794				
H ₂₁ O ₄		1.721	1.647			O ₃ O ₅			2.664		
H ₁₃ O ₄				1.616	1.647	O ₄ O ₅	2.789				
H ₅₁ O ₅	0.984	0.960									
Angles (deg)											
∠(O ₁ H ₂₁ O ₂)	176.7					∠(O ₂ H ₅₁ O ₅)				179.9	
∠(O ₁ H ₁₁ O ₂)					167.6	∠(O ₃ H ₄₁ O ₄)	176.9				
∠(O ₁ H ₁₂ O ₃)				171.7	171.9	∠(O ₃ H ₃₁ O ₅)			168.1		
∠(O ₁ H ₁₁ O ₃)		170.6	166.0			∠(O ₄ H ₅₁ O ₅)	176.5				
∠(O ₁ H ₁₃ O ₄)				171.7	171.7	∠(O ₁ O ₂ O ₃)	110.6				
∠(O ₁ H ₁₁ O ₅)	175.8			176.9		∠(O ₂ O ₃ O ₄)	104.1				
∠(O ₁ H ₁₂ O ₅)					171.9	∠(O ₃ O ₄ O ₅)	107.7				
∠(O ₂ H ₃₁ O ₃)	175.5					∠(O ₄ O ₅ O ₁)	106.2				
∠(O ₂ H ₂₁ O ₄)		168.3	169.5			∠(O ₅ O ₁ O ₂)	104.8				
∠(O ₂ H ₂₁ O ₅)					166.9						

^a Results for the trimer, tetramer, and pentamer cluster are given in parts a, b, and c, respectively. For the pentamer cluster, results are given for two isomers of the "hydrazine-based" (aI and aII) and "disproportionated ion-based" (dpiI and dpiII) cations (see Figure 4). Identification of the atoms is as given in Figures 2–4.

investigated using LSD calculations with self-consistent inclusion of exchange-correlation gradient corrections. The main results of our study may be summarized as follows.

(i) Neutral (H₂O)_n, n ≤ 5, clusters form ground-state quasi-planar cyclic (polygonal) structures, in agreement with ex-

periments.^{1a,31–34} The calculated shortening of the O–O bond distances for increasing water cluster sizes, which has also been observed experimentally,^{1a} is found to be correlated with a decrease in the distances between the (donor) hydrogens (H_d) and the acceptor (O_a) oxygen atoms involved in hydrogen bonds,

TABLE 3: Energetics (in eV) of Neutral and Singly Charged Water Clusters (for Identification of the Various Species See Figures 1–4)^a

	(H ₂ O)	(H ₂ O) ₂	(H ₂ O) ₃	(H ₂ O) ₄	(H ₂ O) ₅
E_b	0.163	0.561	1.053	1.344	
	[0.163] ^b				
E_{HB}	0.163	0.187	0.263	0.269	
$\Delta(\text{H}_2\text{O})$	0.163	0.397	0.492	0.291	
νIP	12.75	11.80	11.03	10.38	9.90
	[12.69] ^b	[11.74] ^b			
aIP	12.66	(a)[10.42] ^b	(a)9.86	(a)9.54	(aI)9.23
	[12.59] ^b	(dpi)[10.64] ^b	(dpi)9.97	(dpi)9.63	(aII)9.29
					(dpiI)9.34
					(dpiII)9.35
$\Delta^+(\text{H}_2\text{O})$	(a)2.34	(a)0.958	(a)0.816	(aI)0.604	
	(dpi)2.11	(dpi)1.069	(dpi)0.835	(aII)0.544	
				(dpiI)0.571	

^a The binding energy of (H₂O)_n is defined as the total energy difference $E_b = E(\text{H}_2\text{O})_n - nE(\text{H}_2\text{O})$; $E_{HB} = E_b/n_{HB}$, where n_{HB} is the number of hydrogen bonds in the cluster. $\Delta(\text{H}_2\text{O})$ and $\Delta^+(\text{H}_2\text{O})$ are the water-molecule removal energies for the neutral and ionized clusters, respectively. νIP and aIP are the vertical and adiabatic ionization potentials of the (H₂O)_n clusters; for the aIP ionization results are given for various final-state charged isomers; for a given cluster size an isomer with a lower aIP value is more stable and the difference between the aIPs of two isomers of a given cluster is the difference between their total energies; for example (H₂O)₂⁺(a) is more stable than (H₂O)₂⁺(dpi) by 0.22 eV. Results for the water monomer and dimer marked by a superscript *b* correspond to calculations¹² with a plane-wave cutoff energy of 158 Ry. ^b Calculated with $E_{\text{cut}} = 158$ Ry.

O_d–H_d•••O_a, accompanied by elongation of the O_d–H_d bonds^{1a} in the donor molecules (for $n = 4$ and 5). The hydrogen bonds for the trimer are highly nonlinear (i.e., average $\angle(\text{O}_d\text{--H}_d\text{•••O}_a)$ value of 152°), implying a high degree of strain, and they tend toward linearity for the tetramer and heptamer. The shortening of the O–O bonds with increasing cluster size is portrayed in a monotonic increase of the hydrogen bond energy in these clusters. The vertical and adiabatic ionization potentials for clusters with $n \geq 2$ are significantly smaller than those of the water molecule, and the aIPs decrease monotonically (see Table 3).

(ii) For the ionized dimer, (H₂O)₂⁺, the ground state is found¹² to be of a hydrazine-like (H₂O–OH₂)⁺ structure (see Figure 1 marked “anti”), with an energy 0.2 eV lower than that of the disproportionated ion, (H₃O)⁺(OH), isomer (see Figure 1).

For larger (H₂O)_n⁺ $n = 3, 4,$ and 5, clusters the low-energy ground-state isomers are predicted to be noncyclic, with the lowest ones forming chainlike structures and containing a hydrazine-like component (see Figures 2b, 3b, and 4b,c), rather than the disproportionated ion (dpi) isomers (see Figures 2c, 3c, and 4d,e). The distances between hydrogen-bonded oxygens in the ionized clusters are contracted in comparison with their values for the corresponding neutral parents. Additionally, the hydrogen bonds in the ionized clusters are more linear than in the neutral ones. These trends correlate with higher values for the energy required to remove a water molecule from the ionized cluster as compared to the value for this process calculated for the corresponding neutral parent (compare $\Delta^+(\text{H}_2\text{O})$ with $\Delta(\text{H}_2\text{O})$, in Table 3).

Finally, we remark that for the ionized water dimer we estimate from BO-LSD-MD simulations that the interoxygen vibrational frequency $\nu(\text{OO})$ is ~ 750 cm⁻¹ for the lowest energy isomer (H₂O)₂⁺(a), while for the disproportionated ion isomer, (H₃O)⁺(OH), $\nu(\text{OO}) \sim 375$ cm⁻¹ (compare to 225 cm⁻¹ in the

neutral dimer). Therefore, measurement of $\nu(\text{OO})$ may serve to identify and distinguish between these ionized dimer isomers.

Acknowledgment. Research was supported by the U.S. DOE (Grant No. DE-FG05-86ER-4234). Computations were performed on Cray computers at the National Energy Research Supercomputer Center at Livermore and the Georgia Institute of Technology Center for Computational Materials Science.

References and Notes

- (1) For recent reviews see: (a) Liu, K.; Cuzan, J. D.; Saykally, R. J. *Science* **1996**, *271*, 877. (b) Castleman, A. W., Jr.; Bowen, K. H., Jr. *J. Phys. Chem.* **1996**, *100*, 12911. (c) Buck, U. In *Clusters of Atoms and Molecules*; Haberland, H., Ed.; Springer Series in Chemical Physics 52; Springer: Berlin, 1994; p 396.
- (2) (a) Haberland, H.; Bowen, K. H. In *Clusters of Atoms and Molecules*; Haberland, H., Ed.; Springer Series in Chemical Physics 56; Springer: Berlin, 1994; p 134. (b) Barnett, R. N.; Cleveland, C. L.; Landman, U.; Jortner, J. *J. Chem. Phys.* **1988**, *88*, 4421, 4429.
- (3) Kaukonen, H.-P.; Barnett, R. N.; Landman, U. *J. Chem. Phys.* **1992**, *97*, 1365.
- (4) Klots, C. E.; Compton, R. N. *J. Chem. Phys.* **1978**, *69*, 1644.
- (5) Haberland, H.; Langosch, H. *Z. Phys. D.* **1986**, *2*, 243.
- (6) Shinohara, H.; Nishi, N.; Washida, N. *J. Chem. Phys.* **1986**, *84*, 5561.
- (7) Ng, C. Y.; Trevor, D. J.; Tiedemann, P. W.; Ceyer, S. T.; Kronebusch, P. L.; Mahan, B. H.; Lee, Y. T. *J. Chem. Phys.* **1977**, *67*, 4235.
- (8) deVisser, S. P.; deKoning, L. J.; Nibbering, N. M. H. *J. Phys. Chem.* **1995**, *99*, 15444.
- (9) (a) See review by Mark, T. D.; Echt, O.; in ref 2a, p 154. (b) Castleman, A. W., Jr. in ref 2a, p 77. (c) Crofton, M. W.; Price, J. M.; Lee, Y. T.; in ref 2a, p 44.
- (10) Stace, A. J. *Phys. Rev. Lett.* **1988**, *61*, 306; *Chem. Phys. Lett.* **1990**, *174*, 103.
- (11) Buck, U.; Winter, M. *Z. Phys. D.* **1994**, *31*, 291.
- (12) Barnett, R. N.; Landman, U. *J. Phys. Chem.* **1995**, *99*, 17305.
- (13) See: Schulz, C. P.; Hertel, J. V.; in ref 2a, p 7.
- (14) Barnett, R. N.; Landman, U. *Phys. Rev. Lett.* **1993**, *70*, 1775, and references therein.
- (15) Barnett, R. N.; Cheng, H.-P.; Hakkinen, H.; Landman, U. *J. Phys. Chem.* **1995**, *99*, 1995, and references therein.
- (16) See refs 3–12 cited in ref 12.
- (17) Good, A.; Durden, D. A.; Kebrale, P. J. *J. Chem. Phys.* **1970**, *52*, 212, 222.
- (18) Tomoda, S.; Achiba, Y.; Kimura, K. *Chem. Phys. Lett.* **1982**, *187*, 197.
- (19) Fehsenfeld, F. C.; Mosesmann, M.; Ferguson, E. F. *J. Chem. Phys.* **1971**, *55*, 2115.
- (20) Kerbralle, P.; Godhole, E. W. *J. Chem. Phys.* **1963**, *39*, 1131.
- (21) Bailey, A. D.; Narcisi, R. S. *J. Geophys. Res.* **1965**, *70*, 3687.
- (22) Wei, S.; Shi, Z.; Castleman, A. W., Jr. *J. Chem. Phys.* **1991**, *94*, 3266.
- (23) See ref 12 and citations to earlier work therein.
- (24) Gill, P. M. W.; Radom, L. *J. Am. Chem. Soc.* **1988**, *110*, 4931.
- (25) Tomoda, S.; Kimura, K. *Chem. Phys.* **1983**, *82*, 215.
- (26) In ref 24 the hydrazine-like (H₂O)₂⁺(a) isomer was found, using high-level quantum chemistry calculations, to be less stable than the disproportionated ion by 37 kJ mol⁻¹, with an isomerization barrier of 33 kJ mol⁻¹.
- (27) Barnett, R. N.; Landman, U. *Phys. Rev. B* **1993**, *70*, 1775.
- (28) Troullier, N.; Martins, J. L. *Phys. Rev. B* **1991**, *43*, 1993.
- (29) Becke, A. D. *Phys. Rev. A* **1988**, *38*, 3098; *J. Chem. Phys.* **1992**, *96*, 2155.
- (30) Perdew, J. P.; Wang, Y. *Phys. Rev. B* **1991**, *44*, 13298; **1991**, *43*, 8911; **1992**, *49*, 13244.
- (31) For the dimer see: Dyke, T. R.; Mack, K. M.; Muentzer, J. S. *J. Chem. Phys.* **1977**, *66*, 498; *Ibid.* **1977**, *66*, 492. Pugliano, N.; Cruzan, J. D.; Loeser, J. G.; Saykally, R. J. *J. Chem. Phys.* **1993**, *98*, 6600.
- (32) For the trimer see: Pugliano, N.; Saykally, R. J. *Science* **1992**, *257*, 1937; Liu, K.; et al. *J. Am. Chem. Soc.* **1994**, *116*, 3507. Liu, K.; et al. *Faraday Discuss.* **1994**, *97*, 35.
- (33) For the tetramer see: Cruzan, J. D.; Braly, J. B.; Kun, L.; Brown, M. G.; Loeser, J. D.; Saykally, R. J. *Science* **1996**, *271*, 59.
- (34) For the pentamer see: Liu, K.; Brown, M. G.; Cruzan, J. D.; Saykally, R. J. *Science* **1996**, *271*, 62.
- (35) Laasonen, K.; Parrinello, M.; Car, R.; Lee, C.; Vanderbilt, K. *Chem. Phys. Lett.* **1993**, *207*, 208.